Published in final edited form as:
Cell. 2010 October 1; 143(1): 84–98. doi:10.1016/j.cell.2010.08.040.

Store-Independent Activation of Orai1 by SPCA2 in Mammary Tumors

Mingye Feng[1], **Desma M. Grice**[3,†], **Helen M. Faddy**[3,†], **Nguyen Nguyen**[2,†], **Sharon Leitch**[1], **Yingyu Wang**[5], **Sabina Muend**[1], **Paraic A. Kenny**[4], **Saraswati Sukumar**[2], **Sarah J. Roberts-Thomson**[3], **Gregory R. Monteith**[3], and **Rajini Rao**[1,*]

[1]Department of Physiology, School of Medicine, The Johns Hopkins University, Baltimore, MD, 21205

[2]Department of Oncology, School of Medicine, The Johns Hopkins University, Baltimore, MD, 21205

[3]School of Pharmacy, The University of Queensland, Brisbane, QLD 4072, Australia

[4]Department of Developmental and Molecular Biology, Albert Einstein Cancer Center, Albert Einstein College of Medicine, Bronx, NY, 10461

[5]Department of Mechanical Engineering, Whiting School of Engineering, The Johns Hopkins University, Baltimore, MD, 21218

SUMMARY

Ca^{2+} is an essential and ubiquitous second messenger. Changes in cytosolic Ca^{2+} trigger events critical for tumorigenesis, such as cellular motility, proliferation and apoptosis. We show that an isoform of Secretory Pathway Ca^{2+}-ATPase, SPCA2, is upregulated in breast cancer-derived cells and human breast tumors, and suppression of SPCA2 attenuated basal Ca^{2+} levels and tumorigenicity. Contrary to its conventional role in Golgi Ca^{2+} sequestration, expression of SPCA2 increased Ca^{2+} influx by a mechanism dependent on the store-operated Ca^{2+} channel Orai1. Unexpectedly, SPCA2-Orai1 signaling was independent of ER Ca^{2+} stores or STIM1 and STIM2 sensors, and uncoupled from Ca^{2+}-ATPase activity of SPCA2. Binding of SPCA2 amino terminus to Orai1 enabled access of its carboxyl terminus to Orai1 and activation of Ca^{2+} influx. Our findings reveal a signaling pathway in which Orai1-SPCA2 complex elicits constitutive store-independent Ca^{2+} signaling that promotes tumorigenesis.

Keywords

Ca2+ signaling; tumorigenesis; basal calcium level; Orai1; STIM1 and STIM2; Ca2+-ATPase activity; store-independent calcium influx

*Correspondence: rrao@jhmi.edu (R. R.).
†These authors contributed equally to this work.

INTRODUCTION

Basal Ca^{2+} concentrations are tightly controlled within a narrow submicromolar range by an array of Ca^{2+} channels and pumps that are susceptible to dysregulation in cancer. Transient changes in cytosolic Ca^{2+} induce downstream signaling events, which regulate a wide range of cellular functions (Berridge et al., 2003; Clapham, 2007; Roderick and Cook, 2008). Ca^{2+} signaling is required for every stage of the eukaryotic cell cycle, including activation and expression of transcriptional factors and cyclin-dependent kinases which are necessary for cell cycle progression (Hogan et al., 2003; Roderick and Cook, 2008), as well as centrosome duplication and separation (Fukasawa, 2007; Matsumoto and Maller, 2002). Crosstalk with other signaling mechanisms, such as the Ras pathway, regulates cell cycle transition and cell proliferation (Cook and Lockyer, 2006; Cullen and Lockyer, 2002). Dynamic regulation of Ca^{2+} signaling is achieved by cooperation of various cellular components including receptors, channels, transporters, buffering proteins, and downstream effectors (Berridge et al., 2003). Thus, inappropriate activation of Ca^{2+} influx channels or downregulation of Ca^{2+} efflux and sequestration mechanisms could increase basal Ca^{2+} to augment Ca^{2+} signaling and tumor cell proliferation. Alternatively, changes that deplete the ER Ca^{2+} store can confer cellular resistance to apoptosis (Monteith et al., 2007).

In most non-excitable cells, depletion of ER stores elicits sustained Ca^{2+} influx by store operated Ca^{2+} (SOC) entry, defining the major Ca^{2+} influx pathway. Upon the stimulation of cell surface receptors, depletion of ER Ca^{2+} results in release of Ca^{2+} from luminal EF hand domains of ER-localized STIM proteins, triggering their translocation to ER-plasma membrane junctions where they bind and activate Orai1, the pore subunit of Ca^{2+} release-activated Ca^{2+} (CRAC) channel, and resulting in refilling of ER stores (Cahalan et al., 2007; Gwack et al., 2007; Lewis, 2007; Vig and Kinet, 2007). Store-operated Ca^{2+} influx is essential for maintaining ER Ca^{2+} content at a precise level, and functions in various physiological processes such as gene transcription, cell cycle progression and apoptosis (Parekh and Putney, 2005). Dysfunction of store-operated Ca^{2+} signaling mediated by STIM and Orai1 leads to inhibition of physiological and pathophysiological activities including breast tumor cell migration and tumor metastasis (Yang et al., 2009), vascular smooth muscle cell proliferation and migration (Potier et al., 2009), and T cell activation and tolerance (Oh-Hora et al., 2008).

The Secretory Pathway Ca^{2+}-ATPases (SPCA) are ATP-powered pumps that deliver Ca^{2+} and Mn^{2+} ions into the Golgi lumen for protein sorting, processing and glycosylation (Durr et al., 1998). In higher vertebrates, including human, this essential function is carried out by the ubiquitously expressed SPCA1 isoform, with orthologs in lower eukaryotes including yeast, nematode and fruitfly (Missiaen et al., 2007). A closely related second isoform, SPCA2, shares similar transport characteristics and appears at first glance to have a redundant role, given its absence in lower eukaryotes (Vanoevelen et al., 2005; Xiang et al., 2005). The limited tissue distribution of SPCA2 includes mammary epithelium, where it is sharply upregulated during lactation. Whereas SPCA1 showed a modest 2-fold induction upon lactation, SPCA2 increased by 35-fold and was localized to the luminal secretory cells of the mammary gland (Faddy et al., 2008).

We hypothesized that transformation of mammary epithelial cells to a cancerous phenotype would be accompanied by dysregulation of Ca^{2+} transporters and their downstream signaling pathways, augmenting proliferation and tumor formation. Furthermore, localized, inappropriate secretion of Ca^{2+} in the absence of calcium buffers, could result in microcalcifications which appear as radiographic “signatures” on mammograms used in diagnosis of breast cancer (Morgan et al., 2005). Although microcalcifications have been extensively used to characterize abnormalities in the breast tissue, a mechanistic understanding

of the source of calcium and the specific pathways that lead to their deposition has remained elusive.

In this study we show that SPCA2 elicits constitutive Ca^{2+} signaling, mediated by Orai1, which correlates with oncogenic activities of mammary tumor cells. Unexpectedly, SPCA2-induced Ca^{2+} signaling was independent of its Ca^{2+} pump activity, and not regulated by store-depletion or STIM proteins. SPCA2 interacted with Orai1 by its N-terminus, and activated Ca^{2+} influx by the C-terminus. These findings reveal a previously unknown Ca^{2+} signaling mechanism in which Orai1 mediates store-independent Ca^{2+} influx, and dysregulation of SPCA2 constitutively activates this pathway leading to oncogenic activity of tumor cells.

RESULTS

Upregulation of SPCA2 Induces Oncogenic Signaling in Mammary Tumor Cells

We investigated the expression of SPCA isoforms in a range of breast cancer-derived and non-malignant mammary epithelial cells by quantitative RT-PCR. In contrast to comparable mRNA levels of SPCA1, SPCA2 was highly upregulated in luminal-like breast cancer-derived cell lines (Figure 1A). Examination of mRNA levels in breast tissue from a small pool of breast cancer patients confirmed this upregulation (Figure 1B) and prompted us to mine data from microarray profiles of 295 primary human breast tumors: highest levels of SPCA2 were found in ERBB2+ tumors, among five transcriptional subtypes (Figure S1). Consistent with mRNA levels, protein expression of SPCA2 was higher in MCF-7 cells, a human breast adenocarcinoma cell line, relative to MCF-10A, a non-malignant human mammary epithelial cell line; in contrast, there was no increase in SPCA1 expression in MCF-7 (Figure 1C). We used lentiviral delivery of shRNA constructs to knock down expression of endogenous SPCA proteins in MCF-7 cells (Figure 1D). Proliferation was inhibited in $SPCA2^{KD}$ cells, with growth rates slower than mock transduced cells, and similar to cells growing in low extracellular Ca^{2+} (~0.1 mM). In contrast, $SPCA1^{KD}$ did not cause this growth phenotype (Figure 1E). The RAS-RAF-MEK-ERK1/2 pathway is known to play an essential role in cell proliferation and survival. Phosphorylation of ERK1/2 drives activation of transcriptional factors and expression of downstream proteins such as cyclin D1, which is essential for completion of G1/S transition (Coleman et al., 2004; Roderick and Cook, 2008). Levels of phospho-ERK and cyclin D1 reduced dramatically in $SPCA2^{KD}$ cells, as well as in cells incubated in low extracellular Ca^{2+}, relative to control cells (Figure 1F).

We examined the effects of depleting endogenous SPCA2 on the transformed phenotype of MCF-7 cells by monitoring growth of cells in soft agar. Fewer and smaller colonies were observed in soft agar seeded with $SPCA2^{KD}$ cells compared to control cells, and normalized results showed a clear reduction of growth in $SPCA2^{KD}$ cells (Figure 1G). Conversely, overexpression of SPCA2 in non-tumorigenic MCF-10A cells conferred the ability to form colonies in soft agar (Fig. 1H) and increased proliferation rate (Figure 1I). We also monitored tumor generation in nude mice injected subcutaneously in the flank with control or $SPCA2^{KD}$ MCF-7 cells. We show that $SPCA2^{KD}$ conferred only sporadic and delayed tumor formation relative to control (Figure 1J).

To determine whether oncogenic activity of endogenous SPCA2 was mediated by Ca^{2+} signaling, we measured basal cytoplasmic Ca^{2+} levels in control MCF-7 and $SPCA2^{KD}$ cells. We showed significant reduction of intracellular Ca^{2+} levels in $SPCA2^{KD}$ cells and in cells growing in low extracellular Ca^{2+}, but not in $SPCA1^{KD}$ cells (Figure 1K). On the other hand, overexpression of SPCA2 in MCF-10A cells significantly increased basal Ca^{2+} concentration (Figure 1L). Although basal Ca^{2+} levels varied between cell lines, these levels could be modulated by SPCA2 expression levels. Thus, SPCA2 appears to play a role in regulating basal

Ca^{2+}, and upregulation of SPCA2 results in constitutive increase of basal Ca^{2+} and cell proliferation associated with oncogenesis.

SPCA2 Elicits Constitutive Ca^{2+} signaling Independent of Transport Function

To investigate the molecular basis of SPCA2-induced Ca^{2+} signaling, we began by monitoring Ca^{2+}-dependent localization of the nuclear factor of activated T cells, NFAT (Crabtree and Olson, 2002; Huang et al., 2006) in HEK293 cells where expression of SPCA2 is relatively low (Figure S2A). In resting cells GFP-tagged NFAT localized exclusively in the cytoplasm. Following treatment with thapsigargin, a blocker of sarco/endoplasmic reticulum Ca^{2+}-ATPases (SERCA), depletion of ER Ca^{2+} resulted in store-operated Ca^{2+} entry, elevation of basal Ca^{2+} level and nuclear translocation of NFAT-GFP in nearly 100% of cells, as expected (Figures 2A–2B). Whereas transient expression of SPCA1 in HEK293 cells did not alter cytoplasmic localization of NFAT-GFP under resting conditions, transient expression of SPCA2 elicited nuclear translocation of NFAT-GFP in ~75% of cells. This was inhibited by store-operated Ca^{2+} channel blockers, miconazole (Clementi and Meldolesi, 1996) and 2-APB (Parekh and Putney, 2005) at the reported concentrations, and in low extracellular Ca^{2+}, indicating Ca^{2+} entry through plasma membrane Ca^{2+} channels. Inhibition of the Ca^{2+}-activated Ser/Thr phosphatase calcineurin by FK506 also prevented nuclear relocalization of NFAT-GFP in SPCA2-transfected cells (Figures 2A–2B). Accordingly, NFAT was predominantly dephosphorylated in TG treated- or SPCA2-expressing cells, but remained phosphorylated in cells transfected with SPCA1 or empty vector, and in FK506 treated-cells (Figure 2C).

These findings were unexpected, given the known function of SPCA2 in pumping Ca^{2+} away from the cytoplasm into Golgi/vesicular stores. To determine whether constitutive Ca^{2+} signaling elicited by SPCA2 was dependent on its Ca^{2+} pumping ability, we generated two variants: mutant D379N lacks the conserved and essential aspartate that is transiently phosphorylated by ATP in the catalytic cycle, and mutant D772A disrupts a conserved and essential Ca^{2+} binding site (Figure 2D) (Wei et al., 2000). Both mutants failed to rescue growth of a yeast strain lacking endogenous Ca^{2+} pumps in BAPTA supplemented medium, consistent with loss of Ca^{2+}-ATPase activity (Figure 2E), but retained ability to elicit constitutive NFAT translocation in HEK293 cells (Figure 2F). Also, mutant D379N induced growth of MCF-10A in soft agar similar to wild type SPCA2 (Figure S2B). Furthermore, introduction of SPCA2, either wild type or D379N mutant, resulted in elevated basal cytoplasmic Ca^{2+} levels in HEK293 cells, relative to cells transfected with empty vector or SPCA1 (Figure 2G). This was reminiscent of the effect of upregulation of endogenous SPCA2 on basal Ca^{2+} levels in MCF-7 cells (Figure 1K). We conclude that SPCA2, but not SPCA1, induces constitutive Ca^{2+} influx and signaling by a mechanism that is independent of its known function as a Ca^{2+}-ATPase.

SPCA2-Mediated Ca^{2+} Signaling Is Store-Independent

To investigate the possibility that SPCA2 could elicit ER Ca^{2+} store depletion leading to constitutive store operated Ca^{2+} entry (SOCE) we examined the status of the ER Ca^{2+} store. YFP-STIM1, the ER localized Ca^{2+} sensor protein, was present in a reticular, ER-like pattern in resting cells, and redistributed to punctae after store depletion with thapsigargin (Liou et al., 2005), as expected (Figure 3A). Transient transfection with SPCA2 did not elicit puncta formation of YFP-STIM1, suggesting that the ER store was not Ca^{2+} depleted (Figure 3A). Next, we directly measured the ER Ca^{2+} content by ionomycin treatment to completely release Ca^{2+} from intracellular stores. In Ca^{2+}-free medium, peak levels of Ca^{2+} released by ionomycin were identical in cells transfected with SPCA2 or empty vector (Figure 3B and Figures S3A–S3B). In a different, independent approach, we used a thapsigargin-insensitive, ER localized Ca^{2+}-ATPase to ensure that intracellular ER stores were replete with Ca^{2+}. N-terminal GFP-tagged SPCA1 partially mislocalizes to the ER (Figure S3C) where it is functional in filling

the stores and preventing nuclear translocation of NFAT-mCherry after thapsigargin treatment (Figure S3D and Figures 3C–3D). Despite co-expression with ER-localized GFP-SPCA1, SPCA2 was capable of eliciting nuclear translocation of NFAT-mCherry (Figures 3C–3D). HA-tagged SPCA1 localizes to the Golgi (Figure S3C) and does not interfere with thapsigargin-induced SOCE, nor with SPCA2-induced nuclear translocation of NFAT-mCherry (Figure 3D), indicating that Ca^{2+} signaling by SPCA2 is also independent of Golgi stores. It was previously reported that knock down of STIM1 or expression of the dominant negative mutant D76A ΔERM blocked SOC signaling (Huang et al., 2006; Roos et al., 2005), as seen by the failure of TG to elicit nuclear translocation of NFAT (Figure 3E and Figures S3E–S3F). Also, knockdown of STIM2, the feedback regulator of cytosolic and ER Ca^{2+} levels, was shown to lower basal Ca^{2+} concentration (Brandman et al., 2007) (Figures S3E and S3G). However, despite expression of dominant negative D76A ΔERM or knockdown of STIM1 and STIM2 expression, either singly or in combination, SPCA2 retained the ability to increase basal Ca^{2+} concentration and cause NFAT-GFP translocation to the nucleus, evidently by a STIM-independent Ca^{2+} signaling mechanism (Figure 3E and Figures S3F–S3G). We showed that SPCA2 expression in HEK293 cells resulted in Ca^{2+} influx from the extracellular medium, as shown by Mn^{2+} quench of intracellular pre-loaded Fura-2 as well as $^{45}Ca^{2+}$ uptake (Figures S4A–S4B). Initial rates of uptake, monitored within the first 60 s, were significantly increased by expression of SPCA2 (Figure 3F and Figures S4D–S4I). Additionally, measurement of $45Ca^{2+}$ efflux and Fura2 fluorescence confirmed that SPCA2-induced elevation of intracellular Ca^{2+} did not result from decreased rates of Ca^{2+} efflux (Figures S4C–S4F). Consistent with these findings, knockdown of endogenous SPCA2 in MCF-7 cells also diminished store-independent Ca^{2+} entry without changing internal Ca^{2+} stores (Figures 3G–3I). Taken together, our results reveal a mechanism for SPCA2-mediated Ca^{2+} signaling that is independent of both ER and Golgi Ca^{2+} stores.

SPCA2 Interacts with Orai1 to Mediate Ca^{2+} Entry

Our results suggested that SPCA2 elicited Ca^{2+} influx through plasma membrane Ca^{2+} channels. Immunofluorescence and cell surface biotinylation showed partial localization of endogenous SPCA2 to the plasma membrane in MCF-7 cells, where it has the potential to elicit Ca^{2+} influx (Figures 4A–4B). Next, we sought evidence for physical interaction between SPCA2 and candidate Ca^{2+} channels. Although SPCA2 mediated Ca^{2+} influx was independent of ER stores, we observed co-immunoprecipitation of the endogenous store-operated channel Orai1 and native SPCA2 in MCF-7 cells (Figure 4C). We verified and extended these findings using epitope-tagged proteins expressed in HEK293 cells: we could document robust co-immunoprecipitation of Orai1-Myc and HA-SPCA2 (Figure 4D). Consistent with the specificity of the Orai1-SPCA2 interaction, HA-SPCA1 did not co-immunoprecipitate with Orai1 (Figure 4D). Similar to endogenous protein, up to 10% of HA-SPCA2 could be labeled by cell surface biotinylation, including both wild type and the pump-inactive D379N mutant; in contrast, SPCA1 was barely detectable (Figure 4E). Surface residence of SPCA2 correlated with total expression levels, and with elevation of basal Ca^{2+} (Figure S5A). We also used cell surface biotinylation to confirm that a portion of SPCA2-complexed Orai1 was found at the plasma membrane (Figures S5B–S5C). Although SPCA2 preferentially interacted with lower molecular weight bands of post-translationally modified Orai1 as has been reported for STIM1 (Park et al., 2009; Vig et al., 2006), we confirmed that all forms of Orai1 reached the plasma membrane where they could be biotinylated (Figure 4B). Epitope-tagged SPCA2 and Orai1 also partially co-localized by confocal immunofluorescence microscopy (Figure S5D). Unlike STIM (Yeromin et al., 2006), interaction between SPCA2 and Orai1 was not affected by store depletion with thapsigargin, consistent with a store-independent regulation of Orai1 function (Figure S5E). Supporting this possibility, neither WT STIM1 nor the constitutively active STIM1 mutant (D76A) (Huang et al., 2006; Liou et al., 2005) was in the same protein complex

as SPCA2 (Figure S5F). These findings point to Orai1 as a likely candidate for mediating SPCA2-regulated, store-independent Ca^{2+} influx in breast cancer cells.

To evaluate this possibility, we suppressed the expression of endogenous Orai1 in MCF-7 cells: $Orai1^{KD}$ lowered basal Ca^{2+} to levels comparable to effects of depleting endogenous SPCA2 (Figure 4F). In addition, $Orai1^{KD}$ in MCF-7 cells suppressed cell proliferation (Figure 4G) and inhibited the RAS pathway, as did $SPCA2^{KD}$ (Figures 4H and S5G). Furthermore, $Orai1^{KD}$ suppressed colony formation in soft agar, to a similar extent as $SPCA2^{KD}$ (Figure 4I), and tumor generation in nude mice (Figure 4J). Simultaneous knockdown of both Orai1 and SPCA2 did not confer additive phenotypes (Figures S5H, S5J and S5K). In MCF-10A cells overexpressing SPCA2, cell transformation and elevation of basal Ca^{2+} level were reversed by knockdown of Orai1, consistent with a role for Orai1 downstream of SPCA2 (Figures 4K–4L and Figure S5L). As expected for a store-independent mechanism of Orai1 activation, depletion of STIM1 (Figures S5M–S5O) or STIM2 (Figures S5I–S5K), the upstream activators of Orai1 in SOCE signaling, did not confer comparable phenotypes in MCF-7 cells. Taken together, our data point to promotion of tumorigenic pathways by SPCA2 in breast cancer cells, mediated by interaction with Orai1.

Amino Terminus of SPCA2 Interacts with Orai1

To dissect the molecular determinants of the SPCA2-Orai1 interaction, we evaluated the efficiency of co-immunoprecipitation between a series of SPCA chimeric proteins and Orai1. In each case, the ability of a chimeric protein to co-immunoprecipitate with Orai1 correlated with ability to elicit NFAT translocation, suggesting that physical interaction between the two proteins was required for Ca^{2+} signaling. Chimeras containing the SPCA2 N-terminus showed stronger binding with Orai1 and more effective NFAT translocation (Figure 5A–5C).

Next, we examined physical interaction between Orai1 and major intracellular soluble domains of SPCA2, including N- and C-termini and the large intracellular loop, which contains the iconic aspartate of P-type ATPases (D379). Of these, only the N-terminus was able to pull down Orai1 (Figure 5D). To further map regions within the SPCA2 N-terminus responsible for binding to Orai1, we performed GST pull downs between Orai1 and a series of SPCA1 and SPCA2 fragments. SPCA1 N-terminus did not bind to Orai1, consistent with an absence of functional interaction between SPCA1 and Orai1 (Figure 5E). A region of 40 amino acids within the N-terminus of SPCA2 was able to effectively interact with Orai1 (Figure 5E; construct SPCA2N-8, aa67–106). Surprisingly, this region was highly conserved between the two isoforms, with ~50% amino acid identity (Figure S6A). We therefore conducted mutational replacement of amino acids in SPCA2 N-terminus with the equivalent residues in SPCA1, and identified four amino acids that together were critical for interaction between SPCA2 N-terminus and Orai1 (Figure 5F). Three-dimensional structure of SPCA2 N-terminus, predicted by I-TASSER server (Wu et al., 2007), suggested that Val71, Thr75 and Ser78 were spatially clustered, whereas Val95 was on the remote side (Figure 5G and Figures S6B–S6C). Finally, we evaluated the effect of Orai1 expression on the intracellular localization of N-terminal fragments of SPCA1 and SPCA2 in HEK293 cells. When expressed alone, both fragments were localized intracellularly, with SPCA1 N-terminal fragment diffusely distributed in the cytosol, and the SPCA2 N-terminus concentrated in the perinuclear region. While the co-expression of Orai1 did not change localization of SPCA1 N-terminus, there was a redistribution of SPCA2 N-terminus to the cell surface, providing additional evidence that the N-terminal domain of SPCA2, but not SPCA1 interacts physically with Orai1 (Figure 5H).

Cooperation of SPCA2 N- and C-termini in Ca^{2+} Signaling

We further investigated the molecular mechanism of SPCA2-activated Ca^{2+} signaling. We noticed that the isolated N-terminus of SPCA2 did not elicit NFAT translocation despite being

able to interact directly with Orai1, while C-terminus was sufficient to induce NFAT translocation when it was linked to 2 or more transmembrane domains and targeted to the membrane (Figure 6A and Figures S7A–S7B). Surprisingly, a similar membrane anchored construct containing SPCA1 C-terminus was also able to activate constitutive Ca^{2+} signaling even though full length SPCA1 could not (Figure 6A). In addition, both SPCA1 and SPCA2 membrane-anchored C-terminal domains physically interacted with Orai1 (Figure S7C). We hypothesized that access of SPCA C-terminus to Orai1 was blocked in the full-length proteins, and binding of SPCA2 N-terminus to Orai1 led to exposure of C-terminus and activation of downstream Ca^{2+} signaling. Analysis of deletion and point mutants of SPCA2 C-terminus identified essential functional residues including several positive charges (lysines and arginines) and a putative PDZ binding domain (Figure 6A and Figure S7D), conserved between human, rat and mouse SPCA proteins (Figure S7E). We then measured intracellular Ca^{2+} concentrations upon expression of SPCA2 C-terminal constructs in HEK293 cells. Basal Ca^{2+} level was elevated dramatically by expression of SPCA2 C-terminus, but remained the same as GST control when lysines (arginines) were mutated or putative PDZ domain was deleted (Figure 6B). N-terminal domain of SPCA2, but not SPCA1, had a dominant negative effect, dramatically inhibiting NFAT translocation induced by full length SPCA2 or the C-terminus (Figure 6C), whereas SOCE was not blocked by SPCA2 N-terminus or full length with C-terminus deleted (SPCA2 Δ924–946)(Figure S7F). Importantly, expression of membrane-anchored SPCA2 C-terminus in MCF-10A cells was able to induce cell transformation, consistent with the fact that it was identified to be the functional domain of SPCA2 and elicited constitutive Ca^{2+} signaling (Figure 6D). STIM1 CRAC activation domain (Park et al., 2009) showed a similar effect, supporting the role of Ca^{2+} signaling in cell transformation (Figures S7G–S7H).

We next expressed various domains of Orai1 as GST fusions, including full-length, N- and C-termini, extra- and intracellular loops together with full length or N-terminus SPCA2. Both N- and C-termini, but not the loops of Orai1 were able to pull down both full length and N-terminus of SPCA2, revealing that SPCA2 and Orai1 interacted within the cytoplasm (Figures 6E–6F). We then mapped subregions of Orai1 N- and C-termini to further explore SPCA2 interaction domains (Figure 6G). GST pull down experiments identified a fragment (aa 48–91) of the Orai1 N-terminus that bound SPCA2 with a higher affinity than the full-length N-terminus. Mutation L273S, previously shown to disrupt coiled-coil domain of the C-terminus of Orai1 (Muik et al., 2008), severely reduced the interaction with SPCA2 (Figure 6G). Taken together, we propose a model for SPCA2 interaction with Orai1 and activation of Ca^{2+} signaling. We suggest that the N-terminus of SPCA2 binds Orai1, resulting in a conformational change and exposure of the C-terminus, which can interact with Orai1 either directly or together with other proteins to activate Ca^{2+} influx (Figure S7I).

DISCUSSION

Role of SPCA2 and Orai1 in Breast Tumorigenicity

Our findings reveal a mechanism for activation of the so-called SOCE channel Orai1 that is independent of ER and Golgi Ca^{2+} stores and sensors. This store-independent mode of endogenous Orai1 activation in breast cancer derived MCF-7 cells underlies constitutive Ca^{2+} signaling, proliferation and anchorage-independent growth and implicates a hitherto unrecognized role for Orai1 in breast tumorigenicity. We also identified a role for SPCA2 in tumorigenicity and revealed a functional link to RAS signaling. The RAS-ERK pathway regulates cell cycle progression and cell proliferation, and it is well known that hyperactivation of the *RAS* gene family correlates with various human cancers (Bos, 1989). GTP-exchange factors (GEFs) and GTPase-activating proteins (GAPs) control activity of RAS by regulating the balance of GTP binding and hydrolysis (Donovan et al., 2002; Downward, 1996). Recent

studies have suggested that GEFs and GAPs can be regulated by different Ca^{2+} signals, such as amplitude of the Ca^{2+} signals and frequency of Ca^{2+} oscillation (Cook and Lockyer, 2006). By monitoring activation of ERK and expression of the downstream protein Cyclin D1, we revealed a correlation between SPCA2 and Orai1-mediated increase of basal Ca^{2+} levels and constitutive activation of RAS signaling in MCF-7 cells, placing SPCA2-Orai1 pathway in the RAS signaling network.

Mechanism of Orai1-Mediated Ca^{2+} Signaling Induced by SPCA2

It has been reported that STIM1 and Orai1 mediate CRAC currents in endothelial cells, and knockdown of either elicits cell cycle arrest (Abdullaev et al., 2008). Another recent study implicated a store-dependent role for Orai1 in cell migration of the metastatic breast cancer line MDA-MB-231, based on a requirement for STIM1 (Yang et al., 2009). We note that SPCA2 expression is very low in MDA-MB-231 (data not shown), consistent with a Ca^{2+} signaling mechanism distinct from the store-independent pathway reported here. While the importance of SOC signaling is well established, the store independent Ca^{2+} signaling described in our study suggests that multiple mechanisms may invoke Orai1 activation. Interaction between SPCA2 and Orai1 was not affected by ER store-depletion and activation of SOC signaling, and SOCE was not inhibited by expression of SPCA2, supporting that SPCA-induced signaling may function independently of SOC pathway and different pools or fine subdomains of Orai1 are involved in the two pathways.

ER-localized Ca^{2+} sensor STIM proteins, which regulate SOCE, did not physically interact with SPCA2 or participate in regulation of SPCA2-Orai1 signaling pathway. In addition, internal Ca^{2+} store content was not depleted by suppression or overexpression of SPCA2. Thus, it remains to be determined how the store-independent, Orai1-mediated mechanism of Ca^{2+} influx is regulated. One possibility is that signaling activity of SPCA2 is regulated by its trafficking between Golgi and plasma membrane. Interaction with Orai1 at cell surface may be dependent on a specific conformation of SPCA2 which could be regulated by kinase-mediated phosphorylation, Ca^{2+} binding or changes in pH between extracellular and Golgi lumen. Removal of a potential PDZ-binding motif in the last four residues of the C-terminal tail of SPCA2 abolished Ca^{2+} signaling, suggesting that interaction with scaffold proteins may be important for activation of this signaling pathway.

Based on the function of a series of chimeras and mutant proteins, we propose a model in which cooperation of N- and C-termini of SPCA2 is required for Orai1-mediated Ca^{2+} signaling. Whereas the N-terminus of SPCA2 binds strongly to Orai1, the C-terminus elicits activation of Ca^{2+} influx. Although the Orai1 binding domain within the SPCA2 N-terminus is highly conserved with the corresponding region of SPCA1, no interaction was detected between SPCA1 N-terminus and Orai1. Replacement of four residues within the minimal Orai1 binding domain of SPCA2 N-terminus (Val71, Thr75, Ser78 and Val95) to the corresponding less hydrophobic or charged residues in SPCA1 abolished the interaction with Orai1. Interestingly, C-terminal constructs of both SPCA isoforms, anchored to the membrane by a minimum of two transmembrane helices, were able to elicit Ca^{2+} influx and signaling. Consistent with this, critical amino acids within the C-terminus were conserved in both isoforms from rat, mouse and human. Therefore, we propose a mechanism in which accessibility of SPCA C-termini is blocked in the full-length protein and binding of the N-terminus to Orai1 is required for functional availability of the C-terminus. Consistent with this hypothesis, we find that expression of the soluble N-terminal domain from SPCA2, but not SPCA1, has a dominant negative effect in blocking activation of Ca^{2+} signaling. Long-range conformational interactions between the N-terminus and other cytosolic domains have been noted in SPCA and other P-type pumps, as well as changes in accessibility of the C-terminal tail (Huster and Lutsenko, 2003; Lecchi et al., 2005; Wei et al., 1999).

Physiological and Pathophysiological Perspectives of SPCA2-Induced Ca^{2+} Signaling

The conventional role of ATP-powered Ca^{2+} pumps is to scavenge and extrude cytoplasmic Ca^{2+} in order to terminate a signal, and as a prerequisite for additional signaling events. Unexpectedly, high levels of expression of the Ca^{2+} efflux pump SPCA2 increased, rather than lowered basal cytoplasmic Ca^{2+} levels and conversely, attenuation of SPCA2 expression was accompanied by a decrease in basal Ca^{2+}. We speculate that this unconventional mechanism may be physiologically important in eliciting high rates of transcellular Ca^{2+} flux during lactation (Lee et al., 2006) and in other Ca^{2+} secreting tissues, including salivary glands and intestinal epithelia, where SPCA2 is expressed at high levels. Total calcium concentration in milk, can reach up to 100 millimolar, five to six orders of magnitude greater than typical cytoplasmic concentrations (~0.1μM). Thus, there must be energy dependent transport processes for effective transcellular movement of Ca^{2+} from blood into milk. In mammary gland, a 30-fold transcriptional increase in the plasma membrane Ca^{2+} pump isoform, PMCA2, is accompanied by apical efflux of Ca^{2+} into milk (Reinhardt et al., 2004). Compared to modest changes in SPCA1 levels, SPCA2 was found to be upregulated during pregnancy (~8-fold), and dramatically upon lactation (~35-fold on day 1). Furthermore, SPCA2 expression was restricted to the luminal cells of lactating glands (Faddy et al., 2008). Our findings raise the possibility that SPCA2 traffics to the basolateral membrane where it can interact with Ca^{2+} channels to elicit Ca^{2+} influx and promote transcellular Ca^{2+} transport.

The unusual role of SPCA2 in activation of Ca^{2+} influx supersedes its ATP-dependent Ca^{2+} sequestering activity and may be a raison d'etre for its redundant expression along with SPCA1, in mammals and higher vertebrates. It is noteworthy that in lower eukaryotes (yeast, worm, fly) and vertebrates (fish), there is only a single ubiquitously expressed SPCA protein, which functions in transporting Ca^{2+} and Mn^{2+} into the secretory pathway. The advent of the SPCA2 gene in higher eukaryotes including frog, mouse, rat and human may correlate with a newly required role in Ca^{2+} signaling. At the molecular level, a longer and divergent N-terminus appears to have endowed SPCA2 with the ability to interact with unique partners, and discrete cell and tissue specific distribution would appear to regulate its function. Whereas in lactation, an exquisitely orchestrated developmental program ensures a coordinated regulation of Ca^{2+} pumps, channels, receptors and buffers, there is emerging appreciation for a pronounced dysregulation of these processes in breast-derived tumor cells. For example, an aberrant switch in heterotrimeric G protein preference by the Calcium Sensing Receptor, CaSR, in breast cancer cells leads to stimulation of cAMP signaling and increased secretion of PTHrP, which in turn is believed to contribute to a "vicious cycle" or feed forward loop of bone metastasis and osteolysis (Mamillapalli et al., 2008). Thus, the upregulation of SPCA2 in the altered signaling environment of tumor cells may result in constitutive Ca^{2+} signaling and cell growth. Inappropriate secretion of Ca^{2+} from these cells, in the absence of calcium buffers, could lead to microcalcifications that are diagnostic of breast cancer. Finally, the separation of signaling function from transport activity in SPCA2, evidenced by our findings, is highly unusual in pumps. An extreme case is SUR1, an ABC transporter that lacks known transport activity but is essential for conferring ATP sensitivity to K_{ATP} channels in insulin secreting pancreatic β cells (Aittoniemi et al., 2009).

In summary, we identified a store-independent SPCA2-Orai1 signaling pathway. Upregulation of SPCA2 led to constitutively active Ca^{2+} signaling and correlated with oncogenic activity in breast cancer. Both SPCA2 and Orai1 emerge as druggable targets of therapeutical potential in the treatment of some breast cancer subtypes.

EXPERIMENTAL PROCEDURES

Materials and additional experimental procedures are described in the Supplemental Data.

SPCA2 Analysis in Human Breast Tumors

A gene expression dataset consisting of the microarray profiles of 295 primary human breast tumors (van de Vijver et al., 2002) was obtained from Rosetta Inpharmatics (Seattle, WA). Tumors were assigned to transcriptional subtypes based on their gene expression profiles (Luminal A [n=88], Luminal B [n=81], Normal-like [n=31], Basal-like [n=46] and ERBB2+ [n=49]) as described (Chang et al., 2005). One probe on the array (annotated as KIAA0703) corresponded to SPCA2. Tumors were grouped by transcriptional subtype and analyzed for SPCA2 expression. Statistical significance between groups was assessed by comparing medians using the Kruskall-Wallis test followed by Dunn's Multiple Comparison Test (Prism version 5, Graphpad Inc.).

NFAT Translocation Assay

Monitoring of nuclear translocation of NFAT was performed 24 hrs post-transfection in HEK293 cells. Fresh medium was added 2 hrs before the start of the experiment. Localization of NFAT-GFP and NFAT-mCherry in cells was examined by fluorescent microscopy. 100–300 cells were manually counted on each coverslip, 3 wells for each condition, and the fraction of cells with nuclear NFAT was calculated. Where indicated, 2 μM thapsigargin was added for 30 minutes, 10 μM miconazole was used for 1 hr, and 50 μM 2-APB was used for 1 hr.

Calcium Imaging and Mn^{2+} quench

Cells were loaded with Fura-2 AM at 1 μg/ml in calcium recording buffer (126 mM NaCl, 2 mM $MgCl_2$, 4.5 mM KCl, 10 mM Glucose, 20 mM Hepes pH 7.4, 2 mM $CaCl_2$; no $CaCl_2$ was added for the 0 Ca^{2+} buffer) for 30 min at RT. After loading, cells were rinsed in same calcium recording buffer without Fura-2 for 20 min. Cells were excited at 340 nm and 380 nm, and Fura AM emission at 505 nm was monitored. Intracellular Ca^{2+} concentration was calculated based on the ratio of 340/380 nm. For Mn^{2+} quench of Fura-2 fluorescence, 0.5mM of Mn^{2+} was added to nominally Ca^{2+}-free buffer. Cells were excited at 360 nm, the isosbestic point of Fura-2, and emission at 505nm was monitored. The average fluorescence of 10 time points (50s) before Mn^{2+} addition was set as 100%.

Construction, Production and Infection of Lentiviruses and Retroviruses

Replication-incompetent lentivirus was used to package shRNA for knockdown in MCF-7 cells and HEK293 cells. Cells were incubated with viruses for 48hrs and selected with puromycin (2–4 μg/ml).

Retroviral gene transfer and expression system (Clontech, Mountain View, CA) was used for stable expression of SPCA2 in MCF-10 cells. SPCA2 gene was cloned into pLXRN vector to package retroviruses. Viruses were collected 48 hrs after transfection, and added to MCF-10A cells. Cells were treated with G418 (400 μg/ml) after 48 hrs infection and selected cells were used to assay proliferation and colony formation in soft agar.

Cell Proliferation Assay

Proliferation was monitored using Celltiter 96® Aqueous One Solution cell proliferation assay kit (Promega, Madison, WI) according to manufacturer's instructions. Briefly, 0.5–1 $\times 10^4$ cells were plated into a 96-well plate. After every 24 hrs, 20 μl of Celltiter 96® Aqueous One Solution reagent was added to each well, and incubated for 2 hrs at 37°C, 5% CO_2. The absorbance at 490 nM was recorded using a 96-well plate reader.

Colony Formation in Soft Agar

Colony formation in soft agar assay was performed using CytoSelect™ 96-well cell transformation assay kit (Cell Biolabs, San Diego, CA). In a 96-well plate, 0.5–1 $\times 10^4$ cells

were resuspended in DMEM containing 0.4% agar and 10% FBS, and layered on to a base agar consisting of DMEM with 0.6% agar and 10% FBS. Following solidification, growth medium was added on to the cell agar layer. 1–2 weeks later, colonies were imaged under the microscope, the agar layer was solubilized and cells were lysed and quantified with CyQuant®GR dye. The plate was read in a FLUOstar Optima plate reader (BMG Labtechnologies) using a 485/520 nm filter set.

Tumor Formation in Nude Mice

Female 4- to 6- week old athymic nude mice (NCI) were received by the animal facility personnel and acclimated at the facility for 2 weeks. Estrogen pellets (SE-121, 0.72 mg/pellet, 60 days release) were obtained from Innovative Research of America. For each animal, a pellet was implanted into the back of the neck through a 1 cm cut and the wound was closed by a wound clip. After 3 days of implantation, the animals were ready to be injected with cells. MCF-7 cells transduced with control or SPCA2 shRNA or Orai1 shRNA were trypsinized and diluted to $1.5–3 \times 10^7$ cells per ml in PBS. 3×10^6 cells per animal were injected subcutaneously into the flank of each of 6–10 mice. The incidence of tumor formation was recorded in each animal once per week, starting 14–18 days after injection. Animal care was in accordance with institutional guidelines. One animal with subsequent tumor necrosis was euthanized, others were sacrificed after 10 weeks of observation.

Immunofluorescence

Cultured HEK293 and MCF-7 cells on coverslips were pre-extracted with PHEM buffer (60 mM PIPES, 25 mM HEPES, 10 mM EGTA, and 2 mM $MgCl_2$, pH 6.8) containing 0.025% saponin for 2 min, and then washed twice for 2 min with PHEM buffer containing 0.025% saponin and 8% sucrose. The cells were fixed with a solution of 4% PFA and 8% sucrose in PBS for 30 min at room temperature, and blocked with a solution of 1% BSA and 0.025% saponin in PBS for 1 hr. Primary antibodies were diluted 1:500 in 1% BSA and incubated with the cells for 1 hr. Alexa Fluor 488 goat anti-rabbit IgG (Invitrogen) and Alexa Fluor 568 goat anti-mouse IgG were used at a 1:1,000 dilution for 30 min. Cells were mounted onto slides using Dako Fluorescent Mounting Medium. Slides were imaged on a Zeiss LSM510-Meta confocal microscope. In Figure 4A, anti-SPCA2 was used. In Figure 5H, anti-SPCA2, anti-SPCA1 and anti-HA were used to detect SPCA2N, SPCA1N and HA-Orai1. In Figure S3C, anti-Myc, anti-SPCA1 and anti-Golgi97 was used to detect Myc-STIM1, HA-SPCA1 and Golgi 97. In Figure S5D, anti-SPCA2 and anti-HA were used to detect Myc-SPCA2 and HA-Orai1. In Figure S7B, anti-GST and anti-HA were used to detect GST-SPCA2C and HA-Orai1.

Co-Immunoprecipitation and GST Pull Down

Co-immunoprecipitation (co-IP) and GST pull down assay in HEK293 cells were performed 24 hrs after transfection. Co-IP in MCF-7 cells for endogenous proteins was performed 24–48 hrs after seeding cells. Cells were lysed in lysis buffer (20 mM Tris-HCl, pH 7.4, 150 mM NaCl, 1 mM Na_3EDTA, 1 mM EGTA, 5 mM $Na_4P_2O_7$, 1 mM Na_3VO_4, 10 mM NaF, supplemented with 1% Triton X-100 and protease inhibitor cocktail (Roche)). 1 / 10 of the lysate was saved as “input”. For co-IP, cell lysate was incubated 1 hr with GammaBind Plus Sepharose (GE Healthcare, Waukesha, WI) for pre-clearance, and 1–4 hrs with antibodies (anti-Myc or anti-SPCA2) at 4°C. GammaBind beads were added and incubated for 1 hr at 4°C. For GST pull down assay, cell lysate was incubated 2hrs with Glutathione Sepharose 4B. Beads were washed using lysis buffer supplemented with 1% Triton X-100 before SDS-PAGE and immunoblotting. 1/2 of the “input” and 1/2 to 1/8 of the Co-IP / pull down fraction were loaded to SDS-PAGE gels. To co-IP cell surface Orai1 with SPCA2, cells were biotin labeled, lysed and immunoprecipitated using anti-SPCA2 antibody. The proteins on the GammaBind beads were eluted with lysis buffer containing 1% SDS, and incubated with neutravidin resin

overnight at RT. Beads were washed in the same buffer. Only the portion of Orai1 that bound to SPCA2 at the cell surface was detected using after SDS-PAGE and immunoblotting. 1/2 of the "input" and 1/2 of the biotinylated fraction were loaded to SDS-PAGE gels.

Functional Complementation in Yeast

Yeast growth assays were performed as described before (Xiang et al., 2005). The yeast strain K616 (*pmr1*Δ*pmc1*Δ*cnb1*Δ) was used as host for plasmids expressing SPCA2. Freshly grown cells were inoculated into each well of 96-well plates at 0.05 $OD_{600\ nm}$. Plates were incubated overnight at 30°C, resuspended by agitation and $OD_{600\ nm}$ was measured using a FLUOstar Optima plate reader.

Three-Dimensional Structure Prediction

I-TASSER method was used to predict 3D-protein structure from the primary amino acid sequence of SPCA2 N-terminus. I-TASSER was ranked as the No.1 server in recent CASP7 and CASP8 experiments (Critical Assessment of protein Structure Prediction).

Article Highlights

SPCA2, but not SPCA1, is highly upregulated in breast cancer cells.

SPCA2 elicits elevation of basal Ca2+ levels mediated by Orai1.

SPCA2 functions independently of its ATPase activity or store-operated Ca2+ entry.

SPCA2-induced Ca2+ signaling is necessary for cell proliferation and tumorigenesis.

Supplementary Material

Refer to Web version on PubMed Central for supplementary material.

Acknowledgments

We thank Dr. Paul Worley and Dr. Guo Huang (Johns Hopkins University) for kind gifts of plasmids expressing Orai1, STIM1, and NFAT. This work was supported by grants from the National Institution of Health GM62142 to R. R., National Health and Medical Research and Cancer Council Queensland 569644 to G. M. and S. R. T., Department of Defense-Center of Excellence Grant W81XWH-04-1-0595 to S. S., laboratory startup funds from the Albert Einstein College of Medicine to P. K., American Heart Association Pre-doctoral fellowship 0815058E to M. F., and American Psychological Association scholarship to H. F. and D. G.

REFERENCES

Abdullaev IF, Bisaillon JM, Potier M, Gonzalez JC, Motiani RK, Trebak M. Stim1 and Orai1 mediate CRAC currents and store-operated calcium entry important for endothelial cell proliferation. Circ Res 2008;103:1289–1299. [PubMed: 18845811]

Aittoniemi J, Fotinou C, Craig TJ, de Wet H, Proks P, Ashcroft FM. Review. SUR1: a unique ATP-binding cassette protein that functions as an ion channel regulator. Philos Trans R Soc Lond B Biol Sci 2009;364:257–267. [PubMed: 18990670]

Berridge MJ, Bootman MD, Roderick HL. Calcium signalling: dynamics, homeostasis and remodelling. Nat Rev Mol Cell Biol 2003;4:517–529. [PubMed: 12838335]

Bos JL. ras oncogenes in human cancer: a review. Cancer Res 1989;49:4682–4689. [PubMed: 2547513]

Brandman O, Liou J, Park WS, Meyer T. STIM2 is a feedback regulator that stabilizes basal cytosolic and endoplasmic reticulum Ca2+ levels. Cell 2007;131:1327–1339. [PubMed: 18160041]

Cahalan MD, Zhang SL, Yeromin AV, Ohlsen K, Roos J, Stauderman KA. Molecular basis of the CRAC channel. Cell Calcium 2007;42:133–144. [PubMed: 17482674]

Chang HY, Nuyten DS, Sneddon JB, Hastie T, Tibshirani R, Sorlie T, Dai H, He YD, van't Veer LJ, Bartelink H, et al. Robustness, scalability, and integration of a wound-response gene expression signature in predicting breast cancer survival. Proc Natl Acad Sci U S A 2005;102:3738–3743. [PubMed: 15701700]

Clapham DE. Calcium signaling. Cell 2007;131:1047–1058. [PubMed: 18083096]

Clementi E, Meldolesi J. Pharmacological and functional properties of voltage-independent Ca2+ channels. Cell Calcium 1996;19:269–279. [PubMed: 8983848]

Coleman ML, Marshall CJ, Olson MF. RAS and RHO GTPases in G1-phase cell-cycle regulation. Nat Rev Mol Cell Biol 2004;5:355–366. [PubMed: 15122349]

Cook SJ, Lockyer PJ. Recent advances in Ca(2+)-dependent Ras regulation and cell proliferation. Cell Calcium 2006;39:101–112. [PubMed: 16343616]

Crabtree GR, Olson EN. NFAT signaling: choreographing the social lives of cells. Cell 2002;109 Suppl:S67–S79. [PubMed: 11983154]

Cullen PJ, Lockyer PJ. Integration of calcium and Ras signalling. Nat Rev Mol Cell Biol 2002;3:339–348. [PubMed: 11988768]

Donovan S, Shannon KM, Bollag G. GTPase activating proteins: critical regulators of intracellular signaling. Biochim Biophys Acta 2002;1602:23–45. [PubMed: 11960693]

Downward J. Control of ras activation. Cancer Surv 1996;27:87–100. [PubMed: 8909796]

Durr G, Strayle J, Plemper R, Elbs S, Klee SK, Catty P, Wolf DH, Rudolph HK. The medial-Golgi ion pump Pmr1 supplies the yeast secretory pathway with Ca2+ and Mn2+ required for glycosylation, sorting, and endoplasmic reticulum-associated protein degradation. Mol Biol Cell 1998;9:1149–1162. [PubMed: 9571246]

Faddy HM, Smart CE, Xu R, Lee GY, Kenny PA, Feng M, Rao R, Brown MA, Bissell MJ, Roberts-Thomson SJ, et al. Localization of plasma membrane and secretory calcium pumps in the mammary gland. Biochem Biophys Res Commun 2008;369:977–981. [PubMed: 18334228]

Fukasawa K. Oncogenes and tumour suppressors take on centrosomes. Nat Rev Cancer 2007;7:911–924. [PubMed: 18004399]

Gwack Y, Feske S, Srikanth S, Hogan PG, Rao A. Signalling to transcription: store-operated Ca2+ entry and NFAT activation in lymphocytes. Cell Calcium 2007;42:145–156. [PubMed: 17572487]

Hogan PG, Chen L, Nardone J, Rao A. Transcriptional regulation by calcium, calcineurin, and NFAT. Genes Dev 2003;17:2205–2232. [PubMed: 12975316]

Huang GN, Zeng W, Kim JY, Yuan JP, Han L, Muallem S, Worley PF. STIM1 carboxyl-terminus activates native SOC, I(crac) and TRPC1 channels. Nat Cell Biol 2006;8:1003–1010. [PubMed: 16906149]

Huster D, Lutsenko S. The distinct roles of the N-terminal copper-binding sites in regulation of catalytic activity of the Wilson's disease protein. J Biol Chem 2003;278:32212–32218. [PubMed: 12794172]

Lecchi S, Allen KE, Pardo JP, Mason AB, Slayman CW. Conformational changes of yeast plasma membrane H(+)-ATPase during activation by glucose: role of threonine-912 in the carboxy-terminal tail. Biochemistry 2005;44:16624–16632. [PubMed: 16342953]

Lee WJ, Monteith GR, Roberts-Thomson SJ. Calcium transport and signaling in the mammary gland: targets for breast cancer. Biochim Biophys Acta 2006;1765:235–255. [PubMed: 16410040]

Lewis RS. The molecular choreography of a store-operated calcium channel. Nature 2007;446:284–287. [PubMed: 17361175]

Liou J, Kim ML, Heo WD, Jones JT, Myers JW, Ferrell JE Jr. Meyer T. STIM is a Ca2+ sensor essential for Ca2+-store-depletion-triggered Ca2+ influx. Curr Biol 2005;15:1235–1241. [PubMed: 16005298]

Mamillapalli R, VanHouten J, Zawalich W, Wysolmerski J. Switching of G-protein usage by the calcium-sensing receptor reverses its effect on parathyroid hormone-related protein secretion in normal versus malignant breast cells. J Biol Chem 2008;283:24435–24447. [PubMed: 18621740]

Matsumoto Y, Maller JL. Calcium, calmodulin, and CaMKII requirement for initiation of centrosome duplication in Xenopus egg extracts. Science 2002;295:499–502. [PubMed: 11799245]

Missiaen L, Dode L, Vanoevelen J, Raeymaekers L, Wuytack F. Calcium in the Golgi apparatus. Cell Calcium 2007;41:405–416. [PubMed: 17140658]

Monteith GR, McAndrew D, Faddy HM, Roberts-Thomson SJ. Calcium and cancer: targeting Ca2+ transport. Nat Rev Cancer 2007;7:519–530. [PubMed: 17585332]

Morgan MP, Cooke MM, McCarthy GM. Microcalcifications associated with breast cancer: an epiphenomenon or biologically significant feature of selected tumors? J Mammary Gland Biol Neoplasia 2005;10:181–187. [PubMed: 16025224]

Muik M, Frischauf I, Derler I, Fahrner M, Bergsmann J, Eder P, Schindl R, Hesch C, Polzinger B, Fritsch R, et al. Dynamic coupling of the putative coiled-coil domain of ORAI1 with STIM1 mediates ORAI1 channel activation. J Biol Chem 2008;283:8014–8022. [PubMed: 18187424]

Oh-Hora M, Yamashita M, Hogan PG, Sharma S, Lamperti E, Chung W, Prakriya M, Feske S, Rao A. Dual functions for the endoplasmic reticulum calcium sensors STIM1 and STIM2 in T cell activation and tolerance. Nat Immunol 2008;9:432–443. [PubMed: 18327260]

Parekh AB, Putney JW Jr. Store-operated calcium channels. Physiol Rev 2005;85:757–810. [PubMed: 15788710]

Park CY, Hoover PJ, Mullins FM, Bachhawat P, Covington ED, Raunser S, Walz T, Garcia KC, Dolmetsch RE, Lewis RS. STIM1 clusters and activates CRAC channels via direct binding of a cytosolic domain to Orai1. Cell 2009;136:876–890. [PubMed: 19249086]

Potier M, Gonzalez JC, Motiani RK, Abdullaev IF, Bisaillon JM, Singer HA, Trebak M. Evidence for STIM1- and Orai1-dependent store-operated calcium influx through ICRAC in vascular smooth muscle cells: role in proliferation and migration. FASEB J 2009;23:2425–2437. [PubMed: 19364762]

Reinhardt TA, Lippolis JD, Shull GE, Horst RL. Null mutation in the gene encoding plasma membrane Ca2+-ATPase isoform 2 impairs calcium transport into milk. J Biol Chem 2004;279:42369–42373. [PubMed: 15302868]

Roderick HL, Cook SJ. Ca2+ signalling checkpoints in cancer: remodelling Ca2+ for cancer cell proliferation and survival. Nat Rev Cancer 2008;8:361–375. [PubMed: 18432251]

Roos J, DiGregorio PJ, Yeromin AV, Ohlsen K, Lioudyno M, Zhang S, Safrina O, Kozak JA, Wagner SL, Cahalan MD, et al. STIM1, an essential and conserved component of store-operated Ca2+ channel function. J Cell Biol 2005;169:435–445. [PubMed: 15866891]

van de Vijver MJ, He YD, van't Veer LJ, Dai H, Hart AA, Voskuil DW, Schreiber GJ, Peterse JL, Roberts C, Marton MJ, et al. A gene-expression signature as a predictor of survival in breast cancer. N Engl J Med 2002;347:1999–2009. [PubMed: 12490681]

Vanoevelen J, Dode L, Van Baelen K, Fairclough RJ, Missiaen L, Raeymaekers L, Wuytack F. The secretory pathway Ca2+/Mn2+-ATPase 2 is a Golgi-localized pump with high affinity for Ca2+ ions. J Biol Chem 2005;280:22800–22808. [PubMed: 15831496]

Vig M, Beck A, Billingsley JM, Lis A, Parvez S, Peinelt C, Koomoa DL, Soboloff J, Gill DL, Fleig A, et al. CRACM1 multimers form the ion-selective pore of the CRAC channel. Curr Biol 2006;16:2073–2079. [PubMed: 16978865]

Vig M, Kinet JP. The long and arduous road to CRAC. Cell Calcium 2007;42:157–162. [PubMed: 17517435]

Wei Y, Chen J, Rosas G, Tompkins DA, Holt PA, Rao R. Phenotypic screening of mutations in Pmr1, the yeast secretory pathway Ca2+/Mn2+-ATPase, reveals residues critical for ion selectivity and transport. J Biol Chem 2000;275:23927–23932. [PubMed: 10801855]

Wei Y, Marchi V, Wang R, Rao R. An N-terminal EF hand-like motif modulates ion transport by Pmr1, the yeast Golgi Ca(2+)/Mn(2+)-ATPase. Biochemistry 1999;38:14534–14541. [PubMed: 10545175]

Wu S, Skolnick J, Zhang Y. Ab initio modeling of small proteins by iterative TASSER simulations. BMC Biol 2007;5:17. [PubMed: 17488521]

Xiang M, Mohamalawari D, Rao R. A novel isoform of the secretory pathway Ca2+,Mn(2+)-ATPase, hSPCA2, has unusual properties and is expressed in the brain. J Biol Chem 2005;280:11608–11614. [PubMed: 15677451]

Yang S, Zhang JJ, Huang XY. Orai1 and STIM1 are critical for breast tumor cell migration and metastasis. Cancer Cell 2009;15:124–134. [PubMed: 19185847]

Yeromin AV, Zhang SL, Jiang W, Yu Y, Safrina O, Cahalan MD. Molecular identification of the CRAC channel by altered ion selectivity in a mutant of Orai. Nature 2006;443:226–229. [PubMed: 16921385]

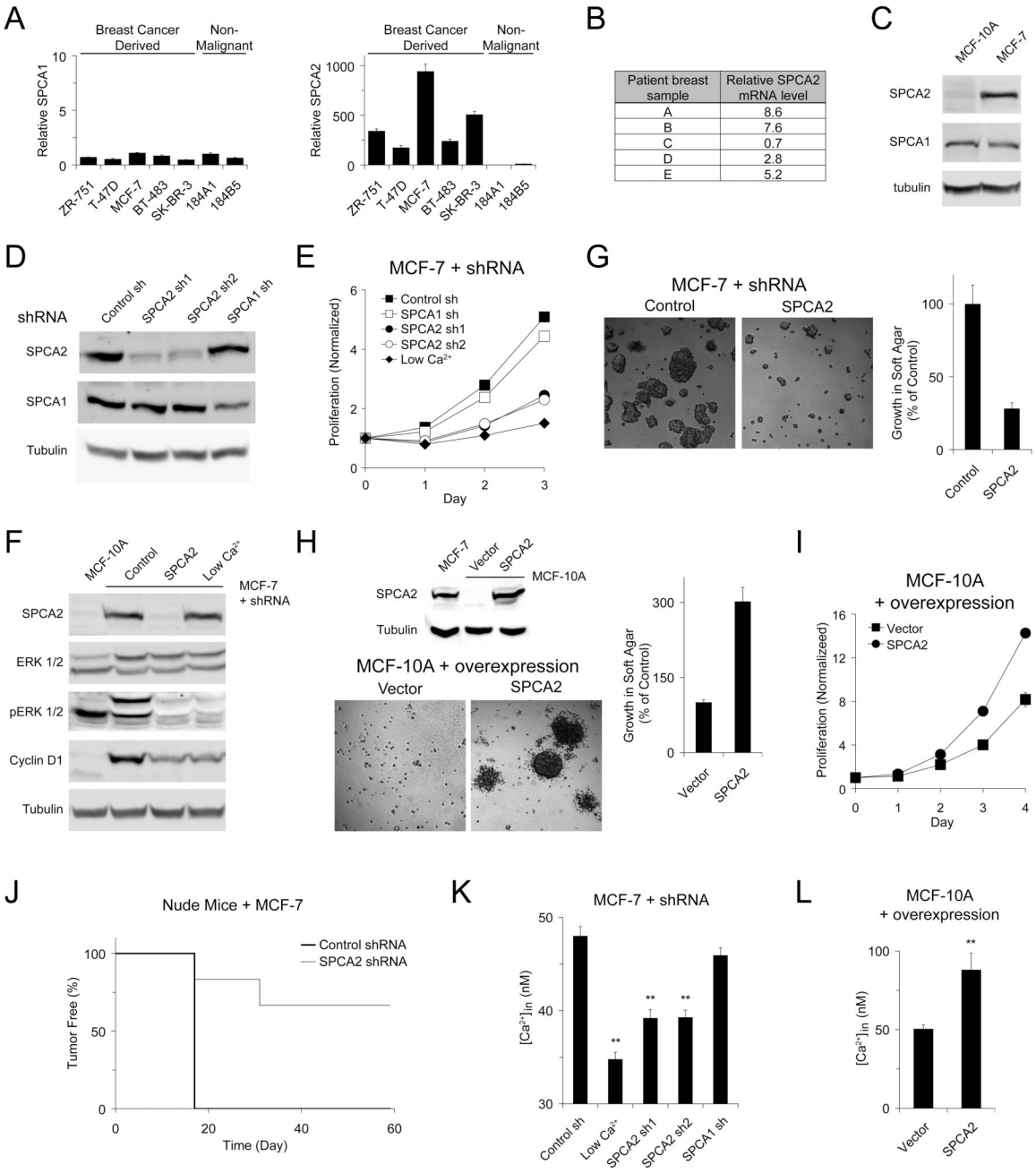

Figure 1. Upregulation of SPCA2 induces oncogenic signaling in mammary tumor cells

mRNA levels were measured by quantitative real-time RT-PCRs and normalized to 18S rRNA in (A) a panel of breast epithelial cell lines relative to 184A1 and (B) in human breast tumor samples compared to matched normal surrounding breast tissue. n = 3 in (A). (C) Immunoblot of SPCA expression in MCF-10A and MCF-7 cells. Immunoblot (D) and normalized proliferation (E) of MCF-7 cells lentivirally transduced with shRNA against SPCA isoforms. n = 3 in (E). (F) Immunoblot of ERK 1/2 phosphorylation and Cyclin D1 expression in MCF-7 cells transduced with shSPCA2. Micrographs and normalized growth of (G) MCF-7 cells with SPCA2 knockdown or (H) MCF-10A cells with SPCA2 overexpression in soft agar. n = 3. Immunoblot showing relative SPCA2 expression levels in (H). (I) Normalized proliferation of

MCF-10 cells with SPCA2 overexpression. n = 3. (J) Tumor incidence in nude mice injected with MCF-7 cells; n = 6, $P = 0.005$ (log-rank test). (K) Basal Ca^{2+} levels in MCF-7 cells with SPCA2 knockdown. From left to right: n = 80, 80, 77, 81, 69. ** $P < 0.01$ (Student's *t*-test). (L) Basal Ca^{2+} levels in MCF-10A cells with SPCA2 overexpression. Vector, n = 23; SPCA2, n = 23. ** $P < 0.01$ (Student's *t*-test). Error bars represent standard error (K and L) or standard deviation (A, E, G, H and I).

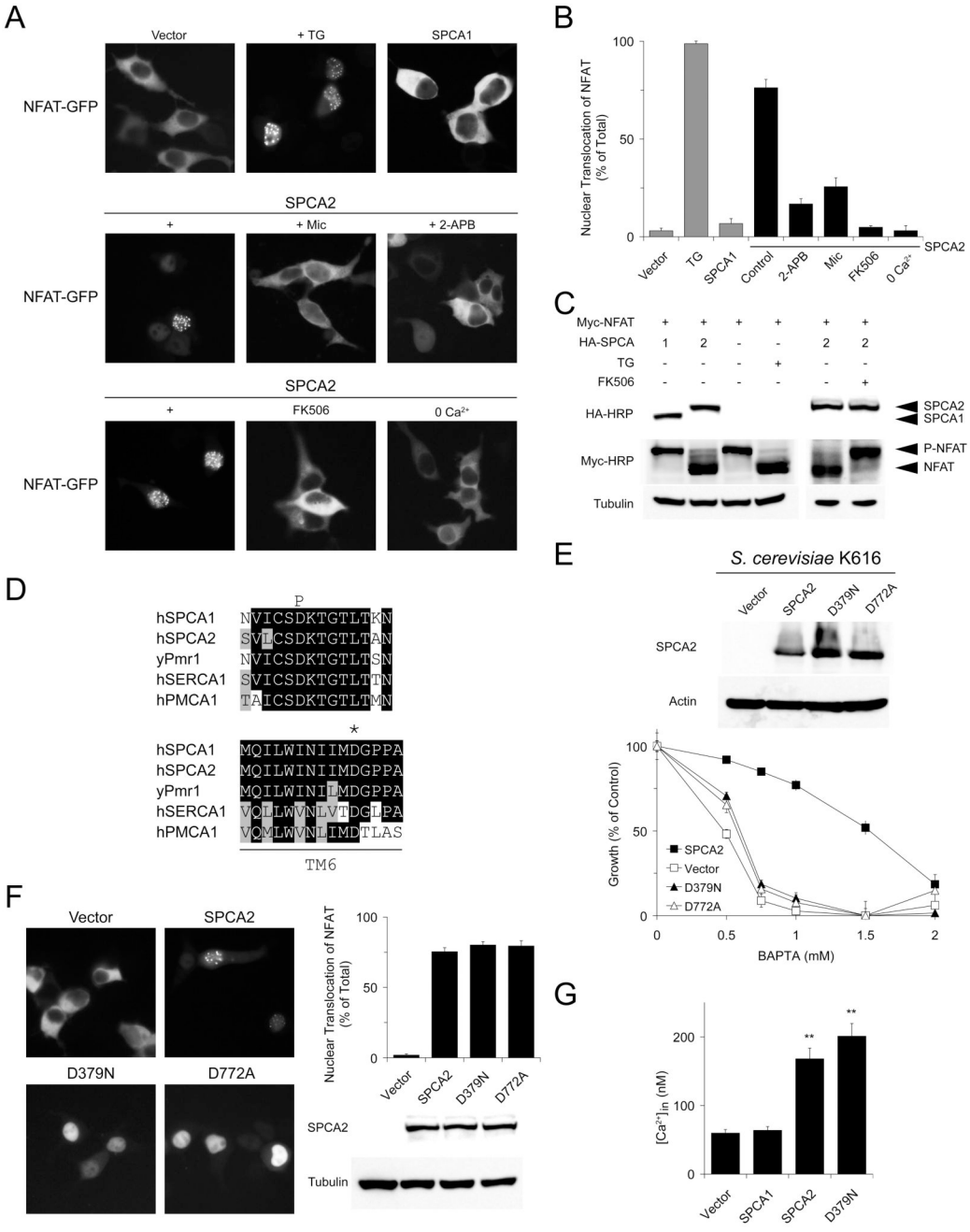

Figure 2. SPCA2 elicits constitutive Ca^{2+} signaling independent of transport function

Representative live images (A) and quantification of nuclear localization (B) of NFAT-GFP in HEK293 cells transfected with SPCA1 or SPCA2, or treated with drugs. n = 3 in (B). (C) Immunoblot showing phosphorylation status of NFAT following expression of SPCA1, SPCA2 or treatment with thapsigargin (TG) or FK506. (D) Alignments showing conserved aspartates in phosphorylation (*P*) domain (D379 in SPCA2) or transmembrane helix 6 (D772 in SPCA2) of P-type Ca^{2+}-ATPases. (E) Immunoblot and normalized growth of yeast K616 expressing SPCA2 or mutants D379N and D772A in BAPTA medium. n = 4. (F) Representative live images, quantification of NFAT translocation in HEK293 cells and immunoblot showing expression of SPCA2 WT or mutants. n = 3. (G) Basal Ca^{2+} levels in

HEK293 cells expressing SPCA1, SPCA2 or D379A mutant. From left to right, n = 57, 47, 46, 44. ** $P < 0.01$ (Student's *t*-test). Error bars represent standard error (G) or standard deviation (B, E and F).

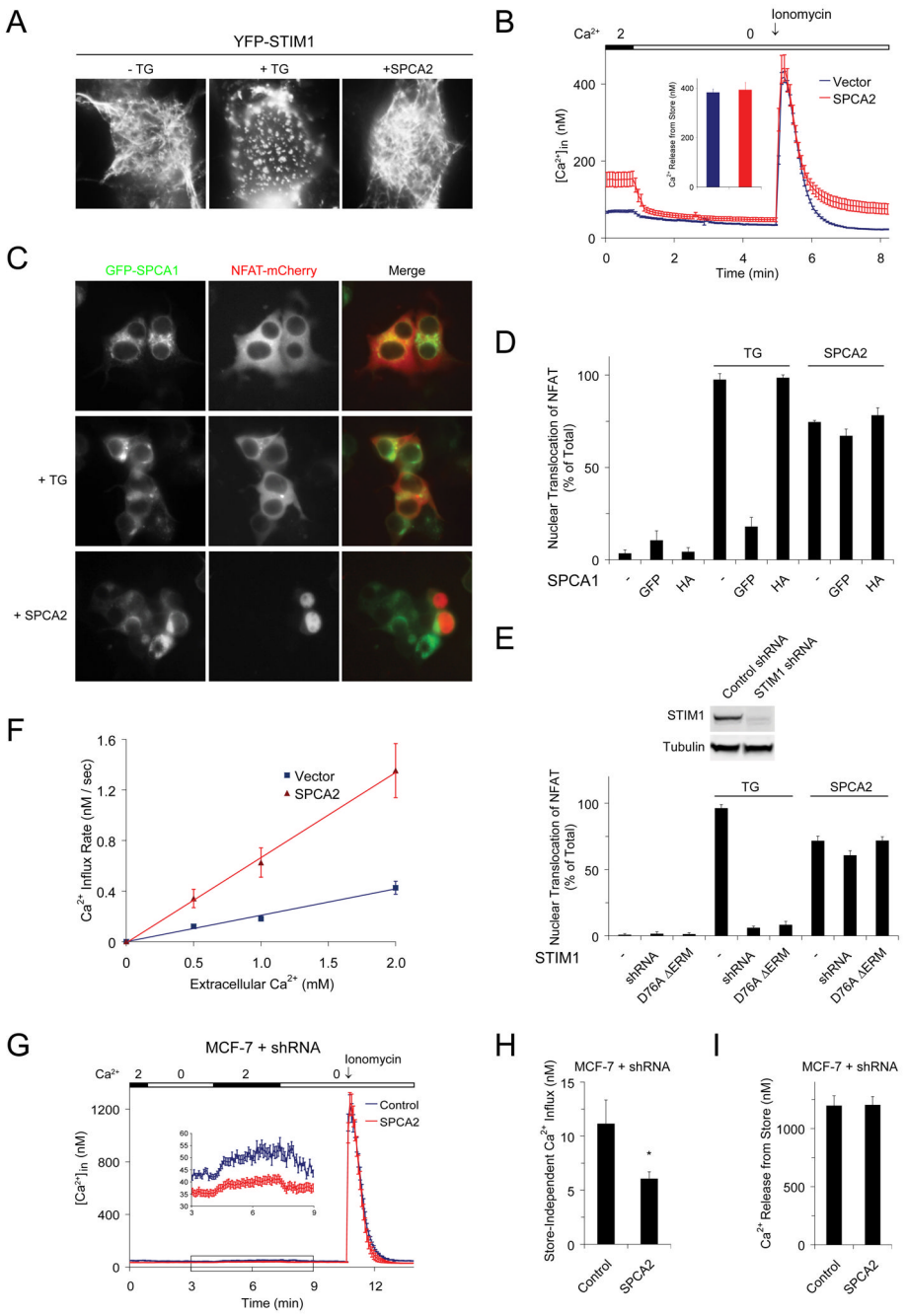

Figure 3. SPCA2 mediated Ca^{2+} signaling is store-independent

(A) Localization of YFP-STIM1 in HEK293 cells following TG treatment or SPCA2 expression. (B) Representative Ca^{2+} traces following emptying of stores with 2 μM Ionomycin in HEK293 cells with or without SPCA2 expression. Vector, n = 40; SPCA2, n = 25. Cells were cultured in low Ca^{2+} medium (~0.1 mM) after transfection, followed by a 30 min incubation in normal Ca^{2+} (2 mM) immediately before calcium imaging experiments to allow restoration of stores (as described in "Supplemental Experimental Procedures - Calcium imaging"). (C) Representative images of GFP-SPCA1 and NFAT-mCherry following TG treatment or SPCA2 expression in HEK293 cells and (D) quantification of nuclear NFAT-mCherry translocation. n = 3 in (D). (E) Quantification of NFAT nuclear translocation

following STIM1 knockdown or expression of dominant negative STIM1 mutant in cells treated with TG or expressing SPCA2. n = 3. (F) Initial rates of Ca^{2+} influx in HEK293 cells with or without SPCA2 expression, calculated from the experiments shown in Figure S4, with 0.5 mM, 1.0 mM or 2.0 mM extracellular Ca^{2+}. Vector: n = 30 (0.5 mM), 25 (1.0 mM), 28 (2.0 mM); SPCA2: n = 28 (0.5 mM), 23 (1.0 mM), 25 (2.0 mM). Representative Ca^{2+} traces (G) and average intracellular Ca^{2+} concentration representing store-independent Ca^{2+} influx (H) and internal Ca^{2+} store content (I) in $Control^{KD}$ and $SPCA2^{KD}$ MCF-7 cells. $Control^{KD}$, n = 36; $SPCA2^{KD}$, n = 30. * $P < 0.05$ (Student's *t*-test). Error bars represent standard error (B, F, G, H and I) or standard deviation (D and E).

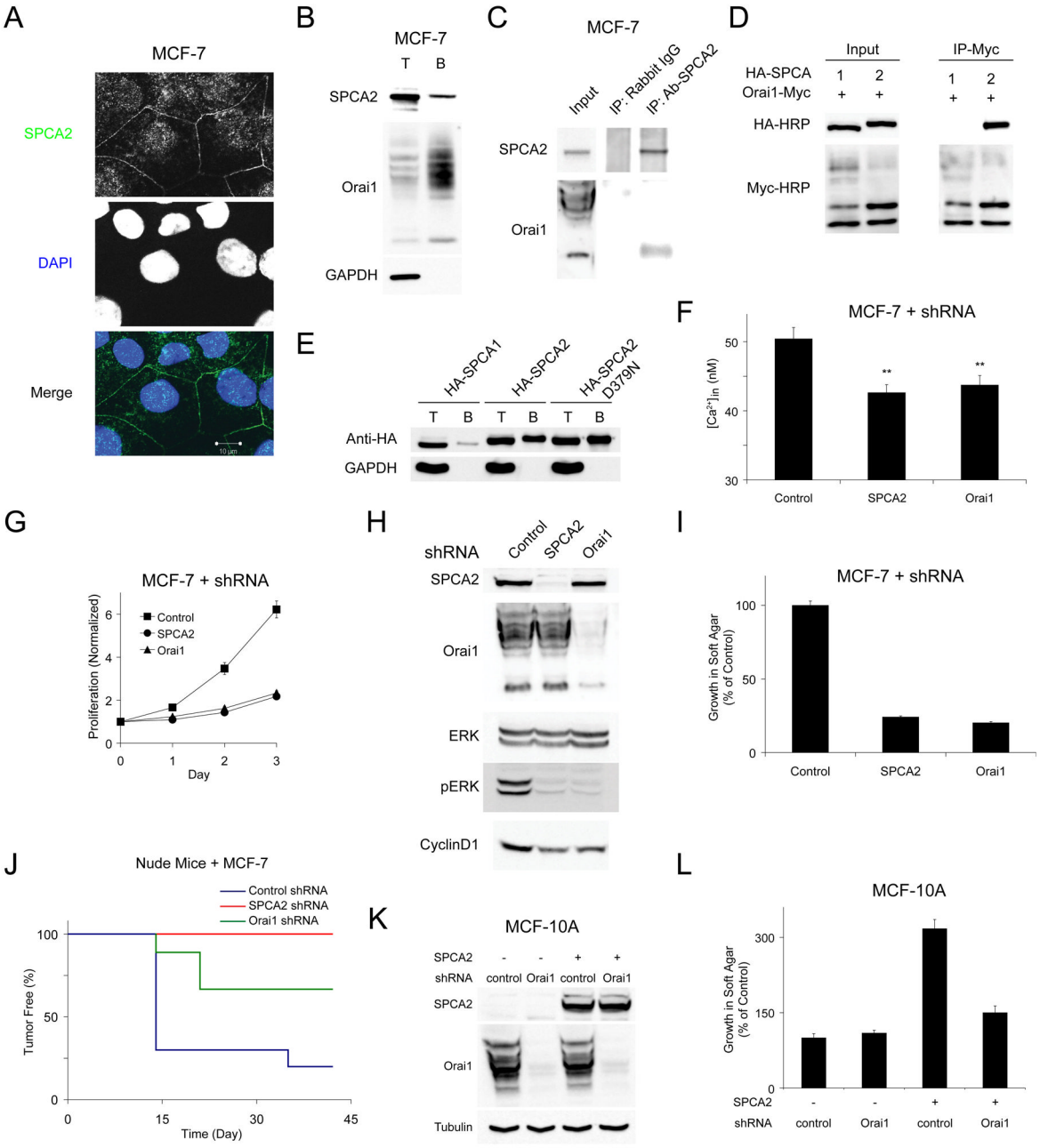

Figure 4. SPCA2 interacts with Orai1 to mediate Ca^{2+} entry

(A) Confocal micrographs of immunofluorescence staining of endogenous SPCA2 in MCF-7 cells showing partial plasma membrane localization. (B) Cell surface biotinylation of endogenous SPCA2 and Orai1 in MCF-7 cells. T and B represent total lysate and biotinylated fraction, respectively. (C) Co-immunoprecipitation of endogenous SPCA2 and Orai1 in MCF-7 cells. (D) Co-immunoprecipitation of HA-SPCA with Orai1-Myc following expression in HEK293. (E) Cell surface biotinylation of HA-tagged SPCA1, SPCA2 or D379N SPCA2 expressed in HEK293. (F) Basal Ca^{2+} in MCF-7 cells after knock down of endogenous SPCA2 or Orai1. $Control^{KD}$, n = 47; $SPCA2^{KD}$, n = 54; $Orai1^{KD}$, n = 52. ** $P < 0.01$ (Student's *t*-test). (G) Normalized proliferation of MCF-7 cells with SPCA2 or Orai1 knockdown. n = 3.

(H) Immunoblot of ERK 1/2 phosphorylation and Cyclin D1 expression in MCF-7 cells with SPCA2 or Orai1 knockdown. (I) Normalized growth of MCF-7 cells with SPCA2 or Orai1 knockdown in soft agar. n = 3. (J) Tumor incidence in nude mice injected with MCF-7 cells; $Control^{KD}$, n = 10; $SPCA2^{KD}$, n = 8, $P = 0.007$ (log-rand test); $Orai1^{KD}$, n = 9, $P = 0.045$ (log-rank test). Immunoblot (K) and normalized growth in soft agar (L) of MCF-10A cells with knockdown of Orai1 in control and cells overexpressing SPCA2. n = 3 in (L). Error bars represent standard error (F) or standard deviation (G, I and L).

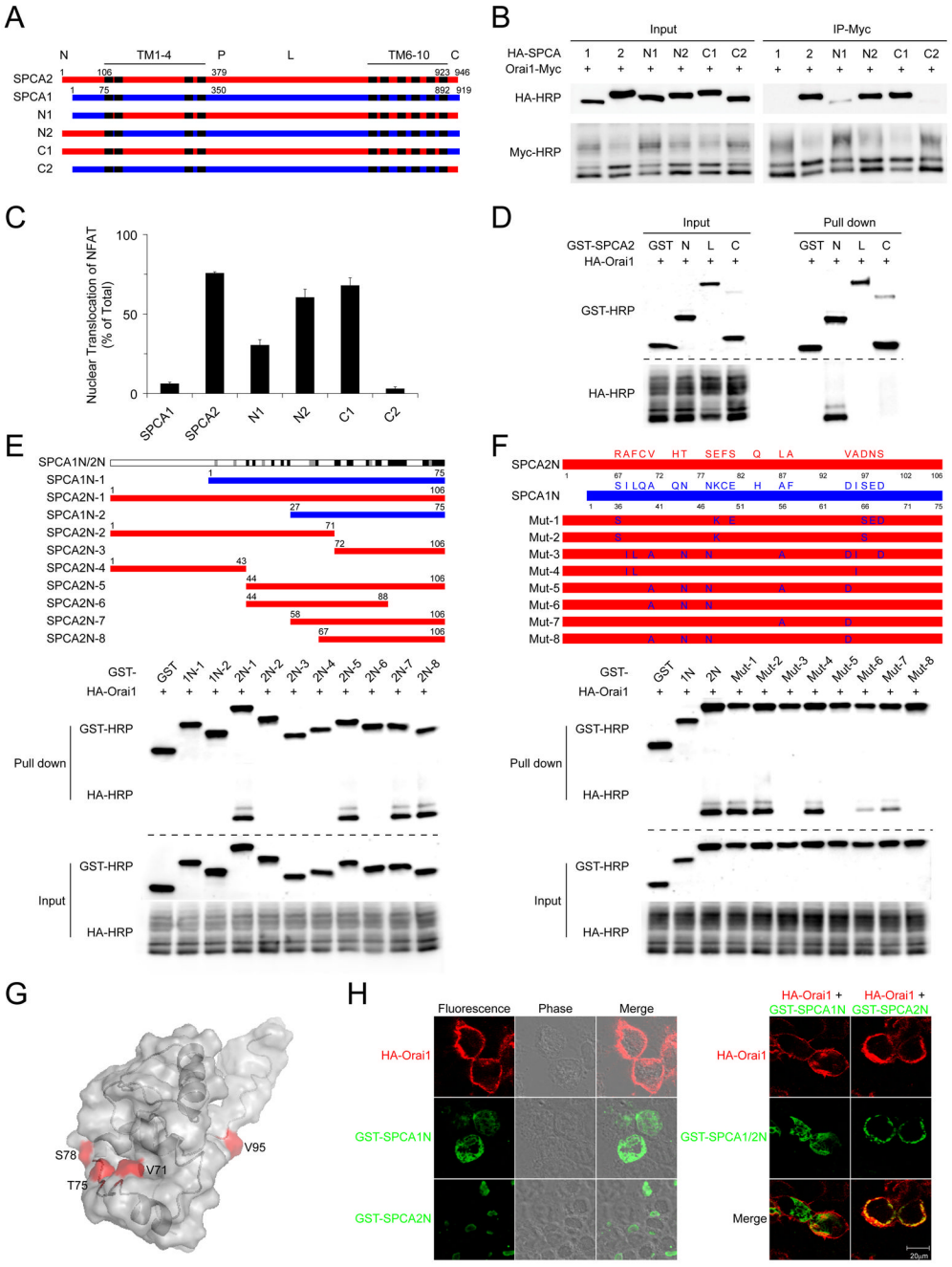

Figure 5. N-terminal domain of SPCA2 interacts with Orai1

(A) Schematic of SPCA chimeras. N1 and C1 have the N- and C-termini of SPCA2 replaced by corresponding regions of SPCA1. N2 and C2 have N- and C-termini of SPCA1 replaced by corresponding regions of SPCA2. “P” indicates the conserved aspartate that is transiently phosphorylated by ATP in the catalytic cycle. “L” represents intracellular loop. (B) Interaction between Orai1 and SPCA chimeras was examined by co-immunoprecipitation in HEK293 cells. (C) Quantification of NFAT nuclear translocation in HEK293 cells expressing SPCA chimeras described in (B). n = 3, error bars represent standard deviation. (D) Interaction between SPCA2 N-terminus (N: aa1–106), intracellular loop (L: aa353–733), C-terminus (C: aa923–946) and Orai1 was examined by GST pull down in HEK293 cells. (E) Mapping of

regions in SPCA1/2 that interact with Orai1. GST-SPCA1/2 N-terminal fragments were coexpressed with HA-Orai1 in HEK293 cells, and interaction with Orai1 was examined by GST pull down. Sequence conservation between SPCA1 and SPCA2 is showed on top, with black, gray and white bars representing identical, similar and different amino acids, respectively, as defined by ClustalW. (F) Screening of SPCA2 N-terminus for amino acids critical for the interaction with Orai1 in HEK293 cells. Point mutations in SPCA2 N-terminus convert amino acids to the equivalent residues in SPCA1 N-terminus. (G) Predicted 3D structure of SPCA2 N-terminus with residues essential for interaction with Orai1 shown in red. (H) Localization of SPCA1 / 2 N-termini, with or without coexpression of Orai1.

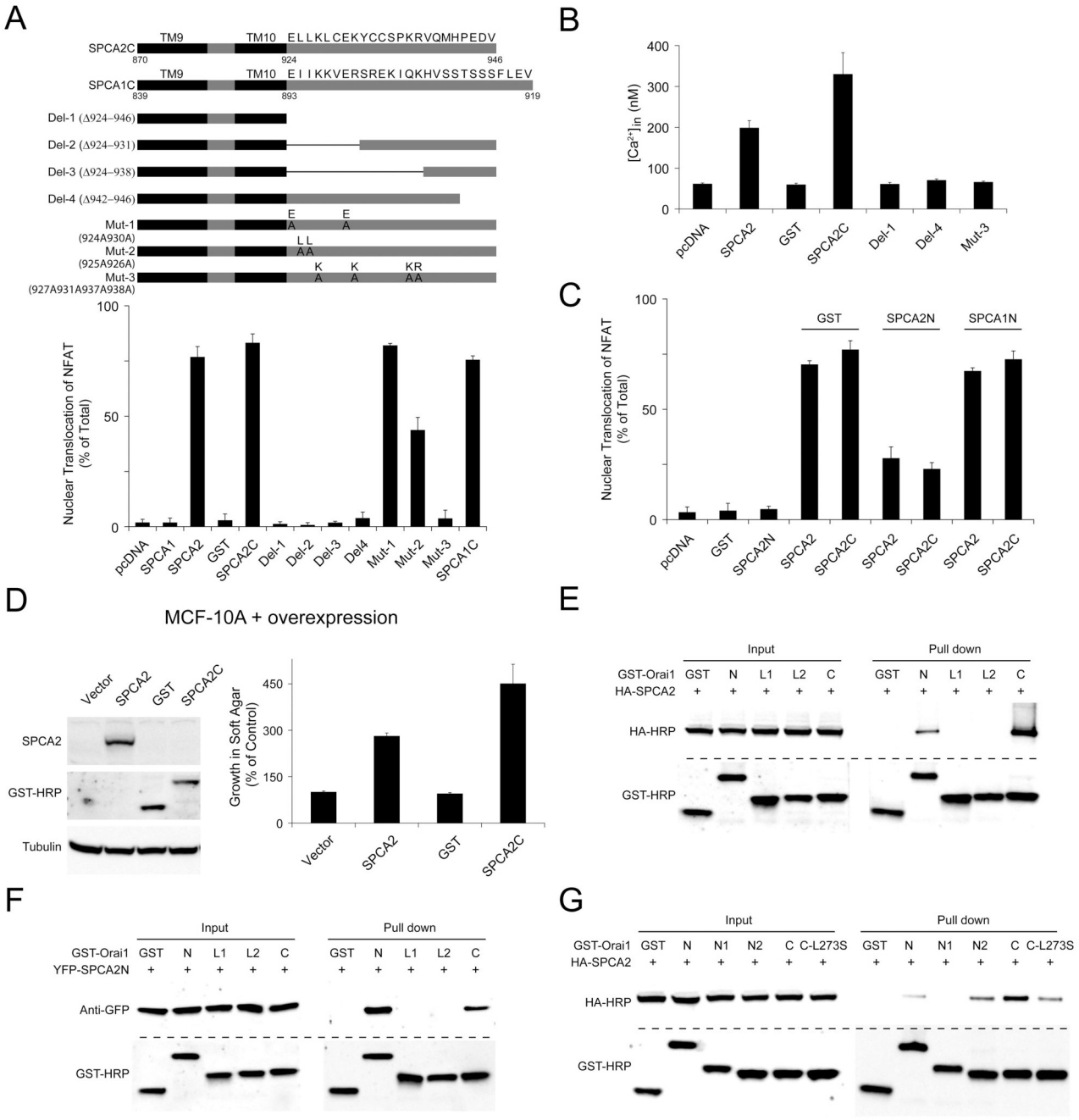

Figure 6. Cooperation of SPCA2 N- and C- terminal domains in Ca^{2+} signaling

(A) SPCA2 C-terminus was sufficient to activate Ca^{2+} signaling. Function of deletion and point mutants of SPCA2 C-terminal domain were examined by NFAT translocation assay in HEK293 cells. Full length SPCA proteins were HA-tagged, all C-terminus fragments shown were GST-tagged. n = 3. (B) Basal intracellular Ca^{2+} concentrations in HEK293 cells, with the expression of GST-tagged deletion and point mutants of SPCA2 C-terminal domain described in (A). From left to right, n = 49, 45, 46, 48, 40, 54, 59. (C) Effects of N-terminal fragments of SPCA proteins on NFAT translocation induced by SPCA2 full length or C-terminal fragment shown in (A). n = 3. (D) Immunoblot and normalized cell growth in soft agar of MCF-10A cells transduced with vector, SPCA2, GST, and membrane-anchored SPCA2

C-terminus (GST-tagged). n = 3. (E and F) Interaction between Orai1 N- (N: aa1–91)), C- (C: aa255–301) termini, intra- (L1: aa141–177), extracellular (L2: aa198–234) loops and SPCA2 full length or N-terminus. (G) Interaction between Orai1 full-length and subregions of N-terminus (N: aa1–91; N1: aa1–47; N2: aa48–91), C-terminus (C: aa255–301), C-terminus mutation (C-L273S) and SPCA2. Error bars represent standard error (B) or standard deviation (A, C and D).